

Article

# Changes of Permeability of Nonwoven Geotextiles due to Clogging and Cyclic Water Flow in Laboratory Conditions

Anna Miskowska <sup>1,\*</sup>, Stanislav Lenart <sup>2</sup> and Eugeniusz Koda <sup>1</sup>

<sup>1</sup> Department of Geotechnical Engineering, Faculty of Civil and Environmental Engineering, Warsaw University of Life Sciences, Nowoursynowska 159 St., 02-776 Warsaw, Poland; eugeniusz\_koda@sggw.pl

<sup>2</sup> Department of Geotechnics and Traffic Infrastructure, Slovenian National Building and Civil Engineering Institute, Dimiceva 12 St., 1000 Ljubljana, Slovenia; stanislav.lenart@zag.si

\* Correspondence: anna\_miskowska@sggw.pl; Tel.: +48-22-5935-213

Received: 1 August 2017; Accepted: 30 August 2017; Published: 1 September 2017

**Abstract:** The use of geotextile filters has been a common application in geo-environmental and geotechnical engineering for decades. The purpose of the present paper is to assess the influence of artificial physical clogging and cyclic water flow on the water permeability characteristics of nonwoven geotextiles used commonly in filter and drainage systems. Despite many studies examining the behavior of soil-geosynthetics, the mechanism of physical clogging is not fully understood yet and remains incompletely defined. Artificial clogging and cyclic water flow tests have been conducted according to a procedure created by the authors. Three nonwoven geotextiles and silty sand were employed in the test series. Hydraulic properties of the tested geosynthetics were determined according to the ISO standard. Filter design criteria are also discussed. The paper also presents the changes of water permeability characteristics due to clogging and cyclic water flow. The results show significant decrease of water permeability coefficients of the tested nonwoven geotextiles after artificial clogging and under cyclic water flow. Furthermore, the clogging mechanism was observed and confirmed by three-dimensional computed tomography.

**Keywords:** nonwoven geotextile; clogging; cyclic flow; permeability; soil

## 1. Introduction

Geosynthetics are modern engineering materials, which have been widely used in soil structures for reinforcing, separation, filtration, and drainage [1–10]. The main functions of geotextile filters are to prevent the movement of fine particles from the base soil and to avoid the development of excessive pore water pressure on the soil–geotextile filter interface. The use of geotextile filters is one of the most common and oldest applications in geo-environmental and geotechnical engineering works [11–14], especially in drainage systems, revetments of channels, armored banks of rivers, and along the coast line [6,15]. Synthetic materials are very cost-effective in comparison to traditional granular drainage layers, easy to transport and install, and reduce the exploitation of natural materials [12,16,17].

However, the selection of particular nonwoven geotextiles for particular places is a critical decision and the hydraulic properties of the material should be measured [18,19], especially, because in drainage and filter applications, nonwoven geotextiles are the first to be in contact with soft, saturated, and fine soils [20].

A geotextile filter includes the geotextile, the interface between the geotextile and the natural soil (filter cake) and the interface between the nonwoven geotextile and the drainage material [21]. For this reason, a geotextile filter should be considered as a filtering zone that evolves over time. Figure 1 presents the evolution of the geotextile filter structure under exploitation.

In some structures, there is a zone that is always subjected to cyclic flow due to the fluctuation of the water table caused by boats, sea waves, or periodic drawdown of water for irrigation purposes.

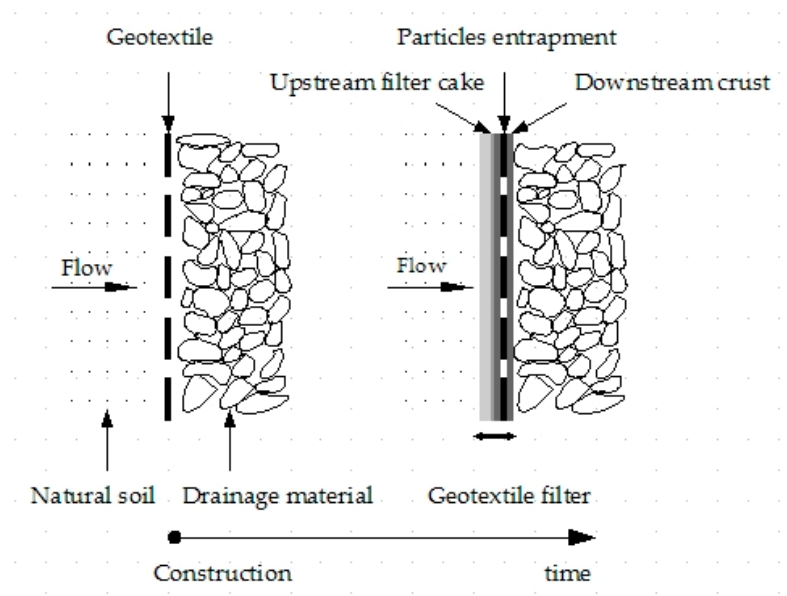


Figure 1. Evolution of a geotextile filter structure over time.

Typical examples are structures consisting of a geotextile filter layer placed on a soil slope, covered with stone armor (Figure 2). When the groundwater table within the revetment is higher than the outside water level, water will flow out from the revetment. On the other hand, when the outside water level is higher, water will flow into the revetment. The percolation rate of water through a soil–geotextile system is a function of the hydraulic gradient. If the geotextile filter does not function well, the structure may fail [6,22–24].

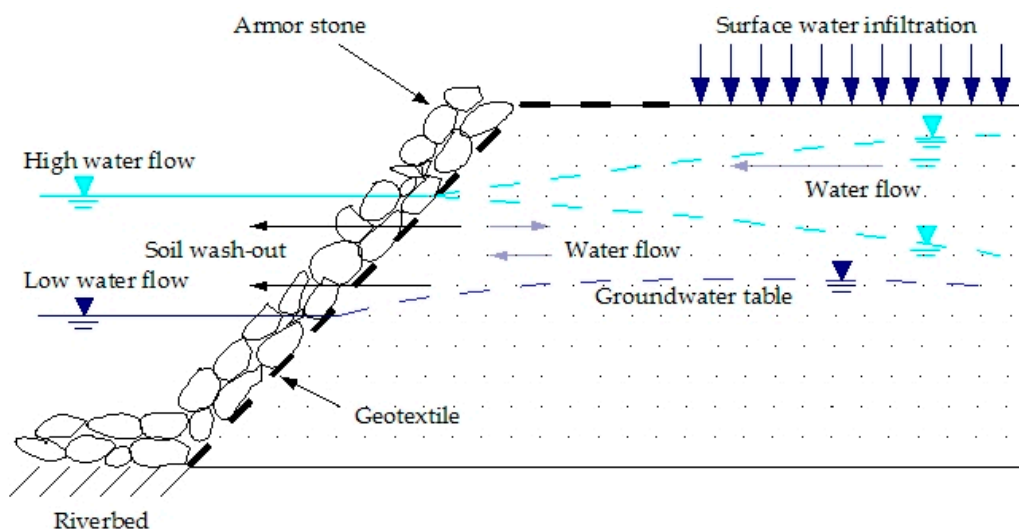


Figure 2. Directions of water flow depending on the water level and the groundwater table.

As a result, the selection of a geotextile filter strongly depends on the design and boundary conditions (applied hydraulic gradient, flow conditions, continuity of the soil–geotextile filter contact interface, shear stresses, and applied vertical effect) and on the geotechnical characteristics of the base soil (grain size distribution, internal stability, relative density, mechanical, and permeability properties).

Current design does not consider all the mentioned factors and is generally based on empirical approaches regarding [11,14,21,25–30]:

- retention—the geotextile should retain the base soil to prevent the piping phenomenon,
- permeability—ensuring the passage of water to guarantee flow and preventing excessive water pressure alongside the filter.

The retention criterion is commonly expressed as

$$O_n \leq xD_n \quad (1)$$

where  $O_n$ — $n$  percent opening size of geotextile (usually  $O_{90}$ );  $x$ —retention ratio dependent on the criterion;  $D_n$ —diameter, for which  $n\%$  in mass of the remaining soil particles are smaller than that diameter (usually  $D_{85}$ ).

The design parameters considered by different authors are variable, chiefly with regard to the indicative diameter of the base soil, the soil relative density, the geotextile opening size, and the type of the geotextile. Therefore, the use of dissimilar retention design criteria must be cautiously evaluated referring to the real in situ design parameters [11,14].

Nevertheless, the permeability criterion is commonly expressed as

$$k_n \geq \lambda k_s \quad (2)$$

where  $k_n$ —coefficient of permeability normal to the plane of geotextile;  $\lambda$ —constant coefficient dependent on the criterion (usually 10–100);  $k_s$ —coefficient of soil permeability.

The permeability criterion includes flow rate and pore pressure requirements. The flow rate requirement consists of comparing the flow rate in a two-layered filter soil filtering system and flow rate in the same soil layer without a filter. The pore pressure requirement means that the presence of the geotextile filter should not increase the pore water pressure in the soil in comparison to the case performed without a filter [31]. Furthermore, the permeability criterion takes into account the blinding and clogging limit states.

Moreover, any design has to be carried out within narrow margins. The approaches are often grouped into “hydraulic” and “geometric” criteria. Hydraulic criteria define the limit value for the hydraulic gradient, at which transport of particles begins. Geometric criteria describe limit values for void diameters to hinder the transport of finer particles through it [23].

Furthermore, clogging criteria are required (the synthetic filter should prevent the clogging process phenomena in the long term). If the nonwoven geotextile filter is not correctly designed, the main limit states of the filtering systems that can occur, leading to the inefficiency of the drainage system, are base soil erosion and synthetic filter external and internal clogging [14,21,32,33].

Blinding (external clogging) occurs when the geosynthetic filters are in contact with internally unstable soils. As a result, if the hydraulic flow moves the base soil particles, these particles accumulate at the base of the soil–geotextile filter interface and a low permeability zone is created. The development of pore water pressures is related to the decrease of permeability at the soil filter interface. Consequently, it affects the structure stability [14]. Clogging is the main mechanism affecting the durability of geotextile filters and is the reduction of the geotextile permeability to a point where flow through it results in the hydraulic system’s non-performance [34]. Physical clogging occurs on the scale of the entire geotextile filter when the particle movement of the base soil leads to the clogging of the geotextile filter pores (Figure 3) [35,36]. Subsequent decrease in effective porosity and interconnectedness of the pore network reduces the hydraulic conductivity of the geosynthetics. The phenomenon results in the decrease of the system drainage capacity [14,21,25,28,37]. The consequent increase of pore water pressure may cause stability problems [11,14].

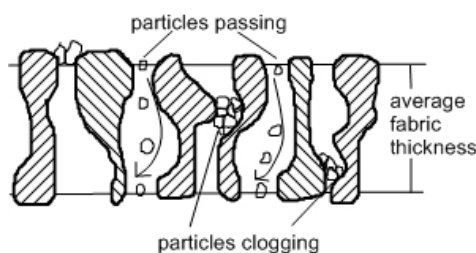


Figure 3. Geotextile clogging.

Moreover, clogging may be caused by accumulation of chemical and biological materials. Biological clogging usually occurs with the formation of surface biofilms, generation of slimes, and the growth of the interconnection of bioconcentrations. Chemical clogging occurs due to the precipitation of iron oxide onto the fibers. These types of clogging are a major concern for drainage in leachate-collection systems [14,16,17,21,35,37–42].

In reference to the issues mentioned above, the main aims of this study are: (1) to create an artificial clogging and cyclic water flow procedure to mimic natural in situ conditions; and (2) to study the influence of clogging and cyclic water flow on the filtration characteristics of nonwoven geotextiles.

## 2. Materials and Methods

### 2.1. Materials

#### 2.1.1. Nonwoven Geotextiles

In this study three types of needle-punched nonwoven geotextiles were employed and will be referred to hereafter as A, B, and C. Table 1 summarizes the main physical and mechanical properties of the applied geosynthetics.

Table 1. Physical and mechanical properties of the tested nonwoven geotextiles.

Geotextile	Mass per Unit Area	Thickness	Opening Size	Tensile Strength	Tensile Strength
	(g/m <sup>2</sup> )	<i>d</i> <sup>1</sup> (mm)	<i>O</i> <sub>90</sub> (μm)	<i>CMD</i> <sup>2</sup> (kN/m)	<i>MD</i> <sup>3</sup> (kN/m)
A	450	4.5	83	27.1	26.7
B	280	2.6	80	24.0	20.3
C	200	2.0	100	14.5	16.0

Notes: <sup>1</sup> geotextile thickness (under 2 kPa normal stress); <sup>2</sup> cross machine direction; <sup>3</sup> machine direction.

In the case of hydraulic properties, the water permeability characteristics of the tested nonwoven geotextiles were determined according to ISO 11058:2010 [43] in the Water Center Laboratory at the Warsaw University of Life Sciences. Figure 4 illustrates the laboratory equipment.

Testing the velocity of flow involved measuring the water flow velocity normal to the plane of a geotextile sample, in a specified time and at an appropriately set water head (70, 56, 42, 28, 14, and additional 3 mm to calculate the water permeability coefficient only). The surface of each of specimen was 19.63 cm<sup>2</sup>. The specimens were placed under water containing a wetting agent at laboratory temperature, and were left to saturate for 24 h. Then the specimens were placed in a cylinder. A supporting mesh was used in the cylinder to avoid deformation of the material by the pressure of water flowing through the holder installed in the device measuring water permeability. The actual volume of water was determined based on the average value from three measurements.

The flow velocity ( $v_{20}$ ) was calculated using the following expressions [43]

$$v_{20} = \frac{V \cdot R_t}{A \cdot t} \quad (3)$$

where  $V$ —water volume measured, ( $\text{m}^3$ );  $R_t$ —correction coefficient for water at the temperature of  $20\text{ }^\circ\text{C}$ , (-) (Equation (4));  $A$ —exposed specimen area, ( $\text{m}^2$ );  $t$ —time measured to achieve the volume  $V$ , (s).

$$R_t = \frac{1,762}{1 + 0,0337 \cdot T + 0,00022 \cdot T^2} \quad (4)$$

where  $T$ —temperature during the test, ( $^\circ\text{C}$ ).

Having compiled the test results, the flow velocity index ( $V_{H50}$ ) was calculated for the water head equal to 50 mm. The coefficient of water permeability ( $k_n$ ) was calculated for 3 mm of the water head [32]

$$k_n = \frac{V \cdot d}{A \cdot t \cdot \Delta h} \quad (5)$$

where  $d$ —thickness of the tested material, (m);  $\Delta h$ —pressure differential under and over the specimen, expressed as the height of the water column, (m).

Statistical flow velocity characteristics for the tested nonwoven geotextile samples A, B, and C before the tests and other hydraulic parameters are shown in Figure 5 and Table 2.

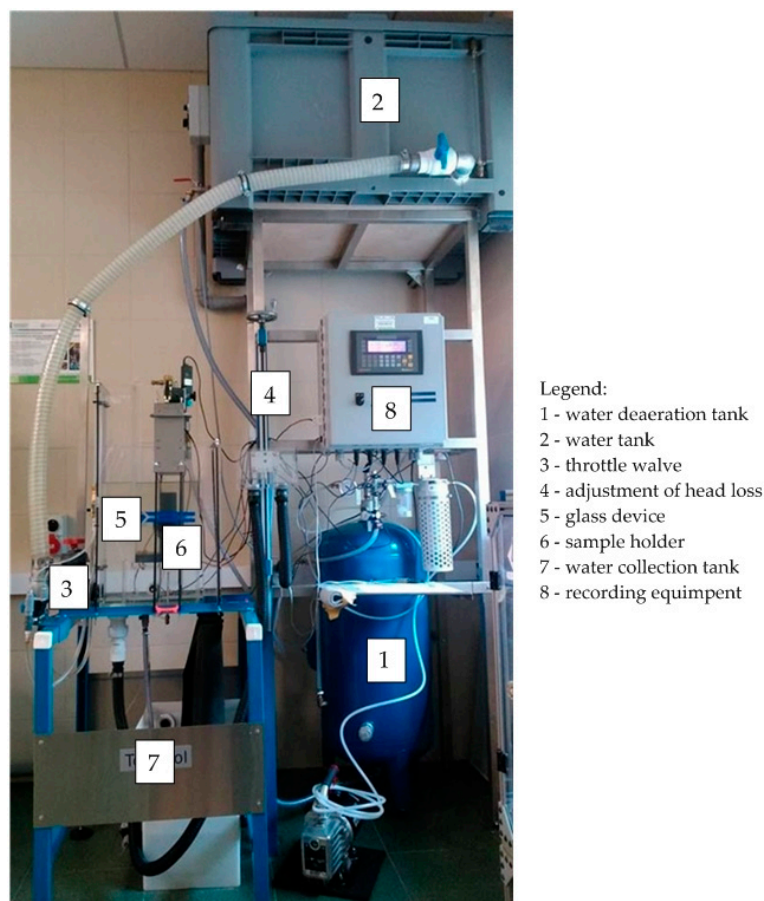


**Figure 4.** Laboratory equipment used for the determination of water permeability characteristics normal to the plane, without load.

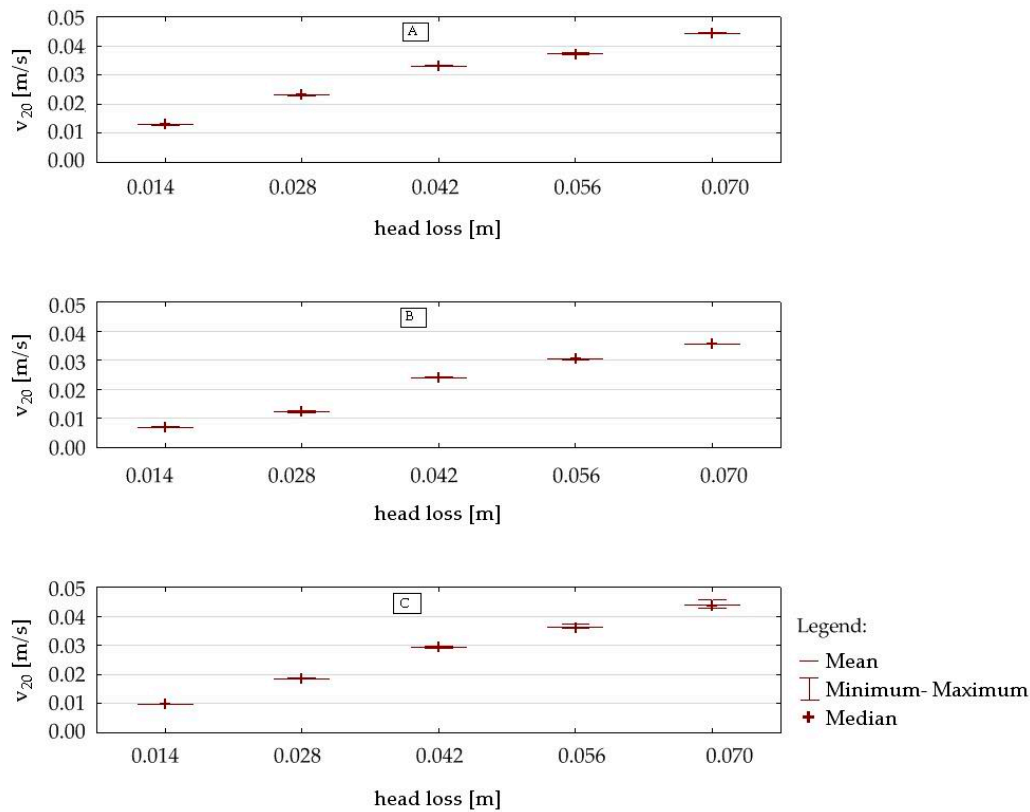


Figure 5. Statistical flow velocity characteristics for the tested nonwoven geotextiles.

The smallest flow velocity index before artificial clogging and cyclic water flow test for nonwoven geotextile B with the smallest characteristic opening size (80  $\mu\text{m}$ ) was determined at 0.026 m/s. In the case of the nonwoven geotextile A with the largest thickness (4.5 mm) and mass (450  $\text{g}/\text{m}^2$ ), the largest flow velocity index and the coefficient of water permeability were determined at 0.035 m/s and 0.0042 m/s, respectively.

Table 2. Summary of statistical analyses of hydraulic properties for the tested nonwoven geotextiles.

Nonwoven Geotextile A						
Head Loss (m)	$v_{20}$ (m/s)					
	Minimum	Quartile 1	Median	Quartile 3	Maximum	Mean
0.014	0.0012738	0.012941	0.012942	0.013100	0.013121	0.012968
0.028	0.022983	0.023059	0.023110	0.023111	0.023318	0.023116
0.042	0.033018	0.033076	0.033100	0.033219	0.022243	0.033169
0.056	0.037000	0.037067	0.037145	0.037199	0.037528	0.037188
0.070	0.044180	0.044316	0.044397	0.044440	0.044592	0.044385
$V_{H50}$ (m/s)	0.035					
$k_n$ (m/s)	0.0042					
Nonwoven Geotextile B						
Head Loss (m)	$v_{20}$ (m/s)					
	Minimum	Quartile 1	Median	Quartile 3	Maximum	Mean
0.014	0.006849	0.007017	0.009838	0.007115	0.007134	0.007033
0.028	0.012124	0.012305	0.018599	0.012496	0.012699	0.012416
0.042	0.023988	0.024016	0.029380	0.024058	0.024186	0.024056
0.056	0.030105	0.030186	0.0360525	0.030389	0.030485	0.030303
0.070	0.035488	0.035499	0.043580	0.035597	0.035688	0.035558
$V_{H50}$ (m/s)	0.026					
$k_n$ (m/s)	0.0013					

Table 2. Cont.

Nonwoven Geotextile C						
Head Loss (m)	$v_{20}$ (m/s)					
	Minimum	Quartile 1	Median	Quartile 3	Maximum	Mean
0.014	0.009835	0.009837	0.009838	0.009839	0.009839	0.009838
0.028	0.018500	0.018589	0.018599	0.018600	0.018700	0.018598
0.042	0.029170	0.029330	0.029380	0.029384	0.029740	0.029401
0.056	0.036000	0.036000	0.0360525	0.036105	0.037189	0.036269
0.070	0.042887	0.043295	0.043580	0.043745	0.045800	0.043861
$V_{H50}$ (m/s)	0.033					
$k_n$ (m/s)	0.0017					

2.1.2. Soil

According to ISO 14688-2 [44], the soil used in the artificial physical clogging and cyclic water flow tests was classified as silty sand (siSa). For this material Table 3 presents the particle size dimensions. Furthermore, the soil was internally unstable (Figures 6 and 7 and Table 4) [45].

Table 3. Particle size characteristics of the soil tested.

Soil	$D_{10}^1$ (mm)	$D_{15}$ (mm)	$D_{50}$ (mm)	$D_{85}$ (mm)	$C_U^2$ (-)	$C_C^3$ (-)
siSa	0.028	0.035	0.17	0.55	8.6	0.54

Notes: <sup>1</sup> diameter, for which  $n\%$  in mass of the remaining soil particles are smaller than that diameter, <sup>2</sup> coefficient of uniformity ( $=D_{60}/D_{10}$ ), <sup>3</sup> coefficient of curvature ( $=D_{30}^2/D_{60}D_{10}$ ).

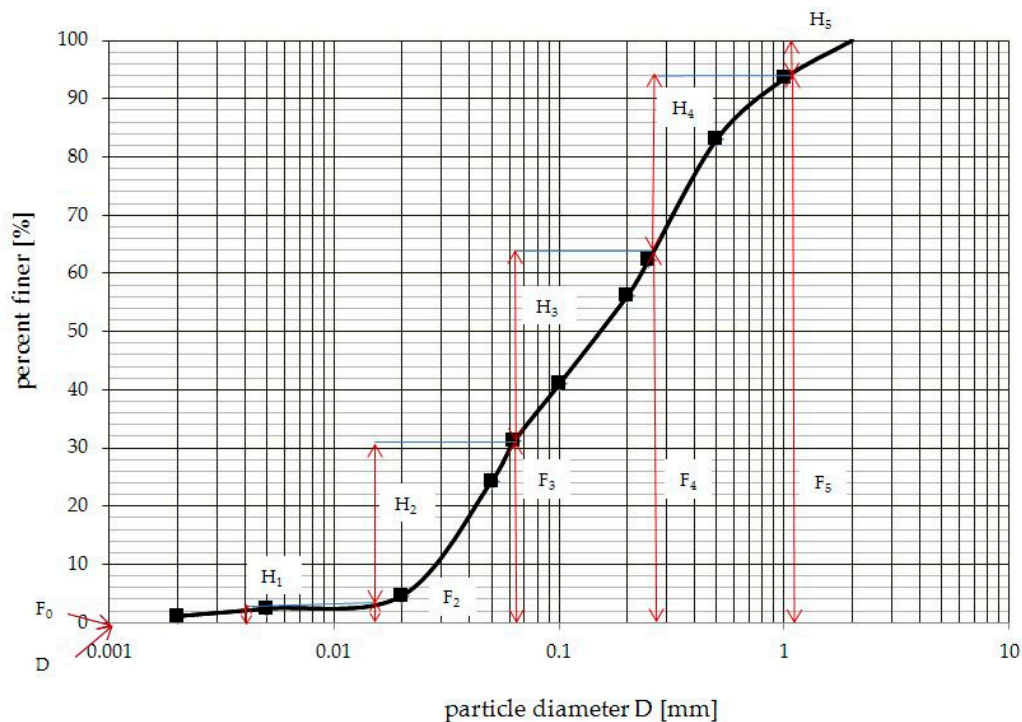


Figure 6. Particle size distribution curve of silty sand and coordinates for the construction of soil internal stability graphs according to Kenney and Lau [45].

Table 4.  $F_n$  and  $H_n$  point coordinates

Particle Diameter $D$ (mm)	Point Coordinate ( $F_n; H_n$ )
0.001	$(F_0; H_0) = (0; 2.0)$
0.004	$(F_1; H_1) = (2; 1)$
0.016	$(F_2; H_2) = (3; 28)$
0.064	$(F_3; H_3) = (31; 33)$
0.256	$(F_4; H_4) = (64; 30)$
1.024	$(F_5; H_5) = (94; 6)$

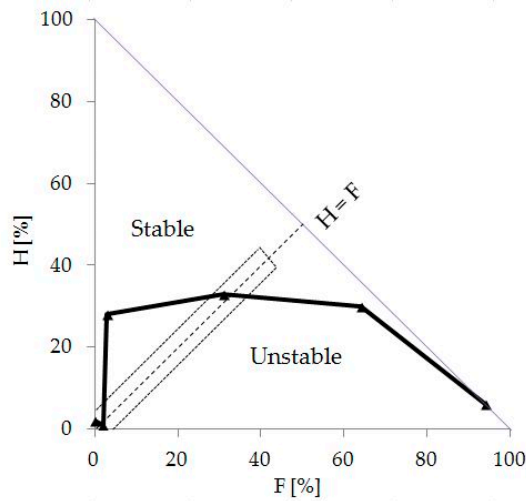


Figure 7. Internal stability of soil graphs according to Kenney and Lau (1985).

2.2. Artificial Clogging Test

Artificial clogging of the tested nonwoven geotextiles was conducted according to a procedure created by the authors in the Geotechnical Laboratory of the Slovenian National Building and Civil Engineering Institute. The laboratory equipment is presented in Figure 8.

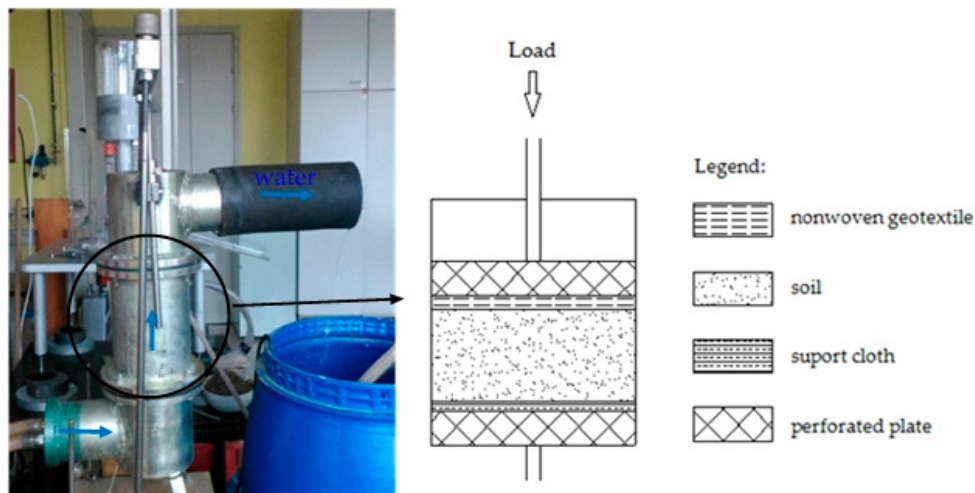


Figure 8. Laboratory equipment for artificial clogging.

The specimen was placed in the central part of this device on a silty sand layer (15 mm thick). Next, water flew through the soil and then through the geotextile at a constant time and water head to allow clogging of the specimen. The load of 10 kPa, representing on site conditions of geotextile

covered with a stone armor, was enough to protect the composite (soil and material) before lifting up. Focus on avoiding empty space at the contact of the composite with the cylinder was very important. In this case, water had to flow through the entire surface of the soil and the tested geosynthetic.

Furthermore, the water flow had to be steady, so that, depending on the physical parameters of the nonwoven geotextiles, a different water head could be used during the test. Necessary value increases of the head loss were from 111 to 300 mm for sample A, from 32.5 to 60 mm for sample B, and from 15.5 to 41 mm for sample C.

Based on the authors' experience [32], the water permeability coefficient of nonwoven geotextiles was determined to check and observe the artificial clogging process after 120 min according to the Equation (5).

In the case of clogged specimens, it is very important to prevent the samples from cleaning before the hydraulic properties are determined. For this reason, the authors recommend the use of a maximum water head of 5 mm in the test. Determination of water permeability normal to the plane of the nonwoven geotextile after clogging and after exploitation according to ISO 11058 [43] is unacceptable because too high of a water head (14–70 mm) results in falsification of the results.

### 2.3. Cyclic Water Flow Test

A cyclic water flow test was conducted according to a procedure created by the authors. The central part (Figure 9a,b) of the laboratory device (Figure 5) was also designed by the authors.

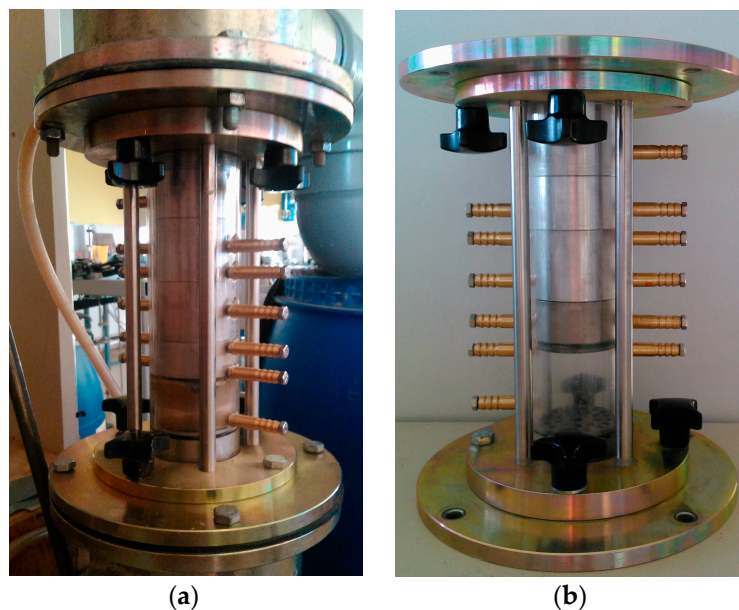


**Figure 9.** Central part of the laboratory equipment for a cyclic water flow test.

The composite of three layers—nonwoven geotextile, soil (50 mm thick layer), and nonwoven geotextile (Figure 9a)—were placed between metal o-rings and perforated plates, which protected the composite before the movement (Figure 9b). Afterward, the water was allowed to flow from the bottom to the top for 30 min and at a constant water head of 100 mm. After this time, the central part of the device was turned around and water flowed for the same time in opposite direction through the composite. The procedure was repeated several times to cause cyclic water flow through the composite and through the geotextile layers within it.

To check and observe the cyclic water flow mechanism after 30, 60, 90, 120, 150, 180, 210, and 240 min of the test, the coefficient of water permeability was determined according to the Equation (5).

Additionally, non-cyclic water flow tests (without rotating the central part) were performed for comparison of the results. In this case the water permeability coefficient of the tested three nonwoven

geotextiles was determined after 60, 120, 180, and 240 min within a water head of 3 mm. The surface of each of specimen was 0.00111 m<sup>2</sup>.

### 3. Results and Discussion

#### 3.1. Artificial Clogging

Nonwoven geotextile samples before and after clogging are shown in Figure 10. Values of hydraulic properties of the tested nonwoven geotextiles after artificial clogging are presented in Table 5.

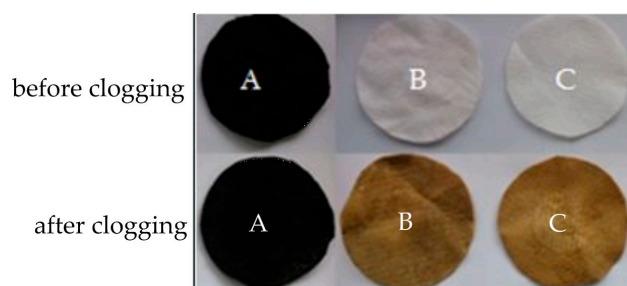


**Figure 10.** Nonwoven geotextiles before (top images) and after 120 min of artificial clogging (bottom images).

**Table 5.** Coefficients of water permeability  $k_n$  of the tested nonwoven geotextile samples.

Type of Geotextile	$k_n$ for Unworn Nonwoven Geotextile (m/s)	$k_n$ for Nonwoven Geotextiles after Artificial Clogging (m/s)	Decrease of $k_n$ (%)
A	0.0042	0.0018	57.1
B	0.0013	0.0002	84.6
C	0.0017	0.0006	64.7

The results show a noticeable reduction of water permeability after the test, indicating possible clogging of the geotextile [32,46,47]. After 180 min of artificial clogging, the coefficient of water permeability decreased even by 84.6% in the case of Sample B.

A nearly identical tendency is presented in the research conducted by Kohata et al. [48] which have confirmed that the coefficient of permeability became small after clogging. Similarly, the results of the studies and observations of filtration behavior of nonwoven geotextiles of Nishigata et al. [49] have shown the influence of particle-size distribution on clogging. The studies of many other researchers [20,28,30,50] have also demonstrated that the flow performance of geotextile filters depends on clogging.

However, it also depends on the physical properties of the materials, such as: opening size, thickness, and mass [26,28,29,32,51]. Sample B was characterized by the smallest characteristic opening size. In turn, Sample A had the largest mass and thickness, therefore the decrease of the coefficient of water permeability was the smallest.

Additionally, stable filtration is guaranteed when the maximum number of the constrictions (dimensionless parameter, which represents the number of “windows” delimited by three or more fibers, in which soil particles could migrate and combines the structural characteristics of the nonwoven material: thickness, porosity, fiber size) does not exceed 40 [25,26]. This confirms that mechanical clogging is strongly connected with the physical properties of nonwoven geotextiles that should be correctly determined before designing. For clogged Specimen B, three-dimensional computed tomography (CT) was carried out (Figure 11).

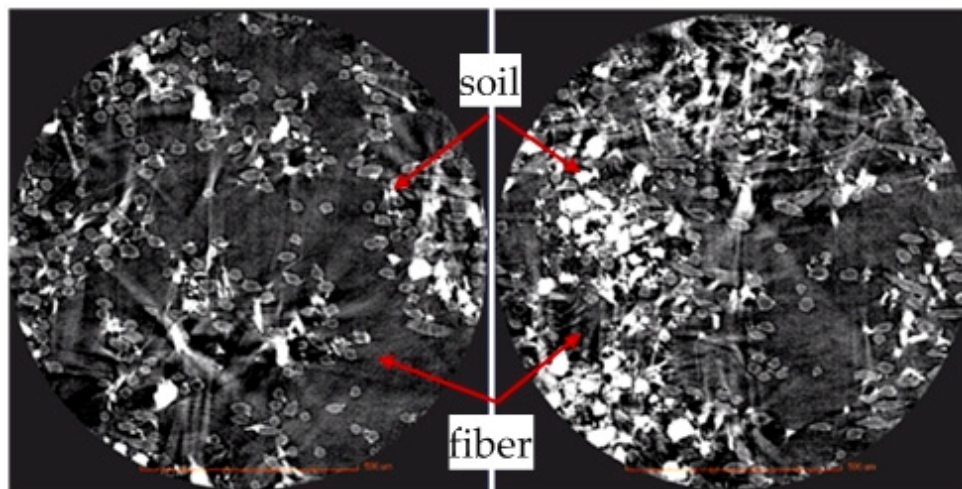


**Figure 11.** Nonwoven geotextile B after artificial clogging.

Analysis of the CT results is difficult because of the heterogeneity of the clogging phenomena, but tests have confirmed that the geotextile pores were clogged by entrapment of soil particles. However, particle entrapment increases the retention capacity of the geotextile filter. This is one of the reasons why filters that fail to meet the retention criteria can still function in an approved manner with regard to the retention of base soil particles [5].

### 3.2. Cyclic Water Flow Test

Cyclic water flow has influence on the hydraulic properties of nonwoven geotextiles and the clogging process. Chen et al. [52] performed filtration tests with cyclic flow and claimed that the fine soil content plays important roles in filtration, clogging, and settlement of the soil–geotextile filter system.

The results of our study show that, with increasing time of the test, the coefficient of water permeability decreased, reaching the minimum value of 0.0011, 0.00014 and 0.00033 m/s for samples A, B, and C, respectively.

In the case of the test without cyclic water flow, geotextiles have not demonstrated the same behavior, since there was a smaller reduction of permeability (Table 6). This indicates that in the case of cyclic water flow, e.g., in coast protection, the clogging process should be closely observed and checked.

The results of the studies by Chen et al. [22] have shown that the fines content has a significant effect on the filtration behavior of a soil–nonwoven geotextile system and cyclic flow has influence on the performance of the geotextile filter. For silty sand, at the beginning of testing the cyclic flow, fine silty particles could migrate and clog within the geotextile. Figure 12 shows the behavior of the tested geotextiles with respect to permeability in the test period studied.

**Table 6.** Coefficients of water permeability  $k_n$  of the tested nonwoven geotextile samples.

Type of Geotextile	$k_n$ for Unworn Nonwoven Geotextile (m/s)	$k_n$ after 240 min of the Cyclic Water Flow Test (m/s)	$k_n$ after 240 min of the Non-Cyclic Water Flow Test (m/s)	Decrease of $k_n$ after the Cyclic Water Flow Test (%)
A	0.0042	0.00110	0.00140	73.8
B	0.0013	0.00014	0.00017	89.2
C	0.0017	0.00033	0.00038	80.6

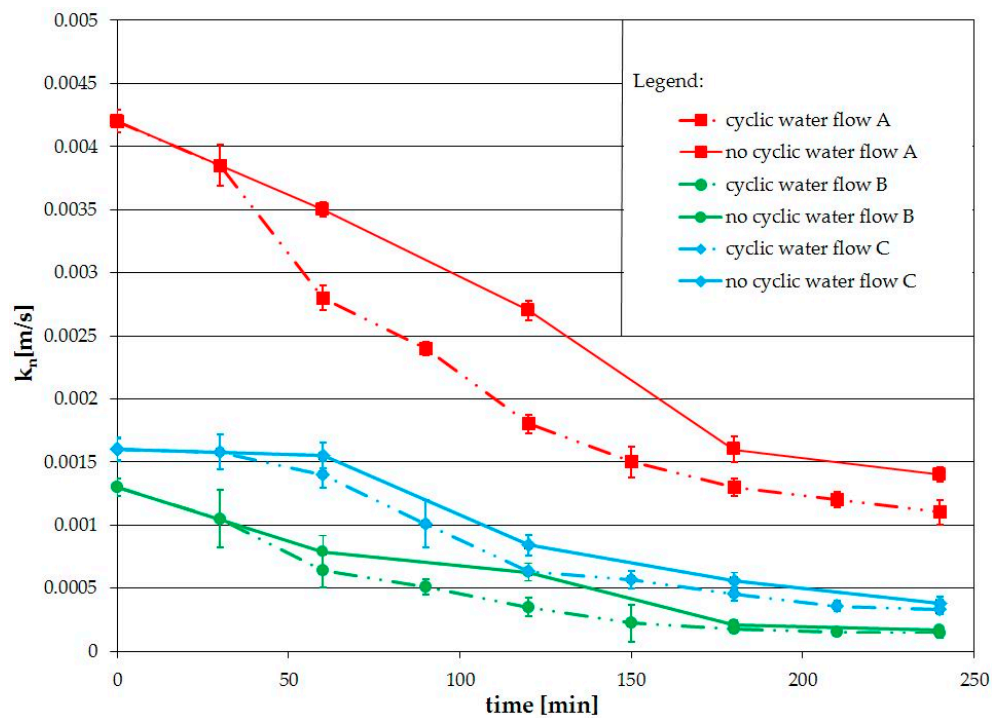


Figure 12. Decreasing of water permeability coefficients with time.

Figure 12 shows the tendency of the tested materials to clog with time, because the coefficients of permeability tend to decrease with time until there is complete blockage of the geotextile voids. The largest decrease of the coefficient of water permeability was observed again for Sample B, and the smallest was observed in the case of Sample A. This confirms that the hydraulic properties of the tested materials depend on the physical parameters. Faure et al. [53] concluded that a thick geotextile with a low number of constrictions should be suitable for bank protection under cyclic flow conditions.

Furthermore, Palmeira and Totto [6] suggested that the presence of a filter reduces the values of maximum pore pressure in the base soil due to damping effects in the case of slopes under cyclic load and water flow, particularly for geotextiles with larger thickness. Three-dimensional CT results are presented in Figure 13. As in the case of the artificial clogging test, CT images have confirmed that the geotextile pores were clogged by soil particles but entrapping of more fine particles was observed.

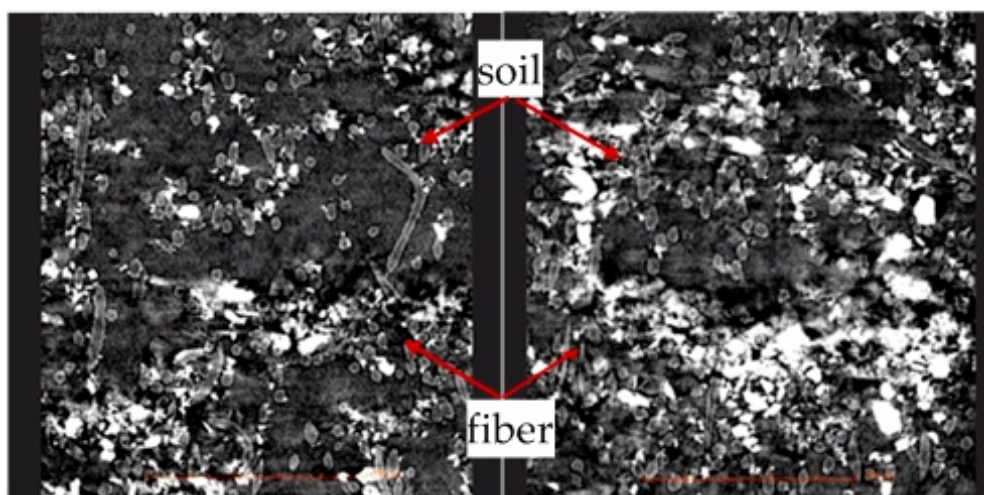


Figure 13. Nonwoven geotextile B after the cyclic water flow test.

#### 4. Conclusions

Understanding the mechanism of clogging is important for knowledge of geotextile filter application in geotechnical engineering especially under cyclic flow. The present research has shown that, under cyclic water flow, physical clogging has larger influence on the decrease of permeability for nonwoven geotextiles in comparison with one-way flow conditions. Furthermore, commonly used design filter criteria, especially clogging criteria, do not exist for cyclic flow conditions. This may lead to faulty design and problems during exploitation. Biological and chemical clogging requires additional research.

Change of hydraulic properties of geotextiles with time depends on the physical parameters of materials, in particular on the mass, thickness, and characteristic opening size.

However, even if some relationship between the different properties of the tested nonwoven geotextiles was observed, it is difficult to establish a linear correlation. The results reported in the present study are based on experimental tests conducted with a limited number of specimens of nonwoven geotextiles. More tests on various geotextiles with different production technologies would be beneficial in the future for a better understanding of the effects of clogging and cyclic flow on the filtration properties of geotextiles.

**Acknowledgments:** This research was performed partially within the COST ACTION TU1202: “Impact of climate change on engineered slopes for infrastructure” during a Short Term Scientific Mission in the Slovenian National Building and Civil Engineering Institute in Ljubljana.

**Author Contributions:** Anna Miszkowska conceived the subject of the paper, performed the literature review, and was responsible for the laboratory tests, statistical data analysis, and writing the conclusions of the research. Stanislav Lenart contributed the materials, designed the device for the cyclic water flow test, and provided the expertise on the research. Eugeniusz Koda was responsible for figure preparation and contributed to the data analysis.

**Conflicts of Interest:** The authors declare no conflict of interest.

#### References

1. Hong, Y.S.; Wu, C.S. Filtration behavior of soil-nonwoven geotextile combinations subjected to various loads. *Geotext. Geomembr.* **2011**, *29*, 102–115. [[CrossRef](#)]
2. Iryo, T.; Rowe, R.K. On the hydraulic behavior of unsaturated nonwoven geotextiles. *Geotext. Geomembr.* **2003**, *21*, 381–404. [[CrossRef](#)]
3. Junquiera, F.F.; Silva, A.R.L.; Palmeira, E.M. Performance of drainage systems incorporating geosynthetics and their effect on leachate properties. *Geotext. Geomembr.* **2006**, *24*, 311–324. [[CrossRef](#)]
4. Liu, L.F.; Chu, C.Y. Modeling the slurry filtration performance of nonwoven geotextiles. *Geotext. Geomembr.* **2006**, *24*, 325–330. [[CrossRef](#)]
5. Palmeira, E.M.; Gardoni, M.G. The influence of partial clogging and pressure on the behavior of geotextiles in drainage systems. *Geosynth. Int.* **2000**, *7*, 403–431. [[CrossRef](#)]
6. Palmeira, E.M.; Totto, J. Behavior of geotextile filters in armoured slopes subjected to the action of waves. *Geotext. Geomembr.* **2015**, *43*, 46–55. [[CrossRef](#)]
7. Palmeira, E.M.; Totto, J.; Araujo, G.L.S. Sagging and filtration behavior of nonwoven geotextiles overlying different bedding materials. *Geotext. Geomembr.* **2012**, *31*, 1–14. [[CrossRef](#)]
8. Park, J.B.; Park, H.S.; Kim, D. Geosynthetic reinforcement of sand-mat layer above soft ground. *Materials* **2013**, *6*, 5314–5334. [[CrossRef](#)] [[PubMed](#)]
9. Raisinghani, D.V.; Viswanadham, B.V.S. Evaluation of permeability characteristics of a geosynthetics-reinforced soil through laboratory tests. *Geotext. Geomembr.* **2010**, *28*, 579–588. [[CrossRef](#)]
10. Scholz, M. Water quality improvement performance of geotextiles within permeable pavement systems: A critical review. *Water* **2013**, *5*, 462–479. [[CrossRef](#)]
11. Cazzuffi, D.; Ielo, D.; Mandaglio, M.C.; Moraci, N. Recent developments in the design of geotextile filters. In Proceedings of the 2nd International GSI—Asia Geosynthetics Conference, Seoul, Korea, 24–26 June 2015.
12. Gardoni, M.G.; Palmeira, E.M. Microstructure and pore characteristics of synthetic filters under confinement. *Géotechnique* **2002**, *52*, 405–418. [[CrossRef](#)]

13. Koda, E.; Szymański, A.; Wolski, W. Field and laboratory experience with the use of strip drains in organic soils. *Can. Geotech. J.* **1993**, *30*, 308–318. [[CrossRef](#)]
14. Moraci, N. Geotextile filter: Design, characterization and factors affecting clogging and blinding limit states. In Proceedings of the 9th International Conference on Geosynthetics, Guarujá, Brazil, 23–27 May 2010; pp. 413–435.
15. Recio, J.; Oumeraci, H. Hydraulic permeability of structures made of geotextile sand containers; Laboratory tests and conceptual model. *Geotext. Geomembr.* **2008**, *26*, 473–487. [[CrossRef](#)]
16. Palmeira, E.M.; Remigio, A.F.N.; Ramos, M.L.G.; Bernardes, R.S. A study on biological clogging of nonwoven geotextiles under leachate flow. *Geotext. Geomembr.* **2008**, *26*, 205–219. [[CrossRef](#)]
17. Vieira, J.L.; Abramento, M.; Campos, M.V.W. Experimental study of clogging in drainage systems. In Proceedings of the 9th International Conference on Geosynthetics, Guarujá, Brazil, 23–27 May 2010; pp. 1145–1148.
18. Nahar, K.; Ferdous, W.; Mofiz, S.A.; Ferdous, K. A simplified mechanism for the vertical permeability test of geo-textile. *Int. J. Civ. Environ. Eng.* **2010**, *10*, 29–33.
19. Paul, P.; Tota-Maharaj, K. Laboratory studies on granular filters and their relationship to geotextiles for stormwater pollutant reduction. *Water* **2015**, *7*, 1595–1609. [[CrossRef](#)]
20. Faure, Y.H.; Baudoin, A.; Pierson, P.; Plé, O. A contribution for predicting geotextile clogging during filtration of suspended solids. *Geotext. Geomembr.* **2006**, *24*, 11–20. [[CrossRef](#)]
21. Veylon, G.; Stoltz, G.; Mériaux, P.; Faure, Y.H.; Touze-Foltz, N. Performance of geotextile filters after 18 years' service in drainage trenches. *Geotext. Geomembr.* **2016**, *44*, 515–533. [[CrossRef](#)]
22. Chen, R.H.; Ho, C.C.; Hsu, C.Y. The effect of fine soil content on the filtration characteristics of geotextile under cyclic flows. *Geosynth. Int.* **2008**, *15*, 95–106. [[CrossRef](#)]
23. Heibaum, M. Geosynthetics for waterways and flood protection structures—Controlling the interaction of water and soil. *Geotext. Geomembr.* **2014**, *42*, 374–393. [[CrossRef](#)]
24. Peng, R.; Hou, Y.; Zhan, L.; Yao, Y. Back-analyses of landfill instability induced by high water level: Case study on Shenzhen landfill. *Int. J. Environ. Res. Public Health* **2016**, *13*, 126. [[CrossRef](#)] [[PubMed](#)]
25. Giroud, J.P. Granular filters and geotextile filters. In Proceedings of the 2nd International Conference Geofilters, Montréal, QC, Canada, 29–31 May 1996; pp. 565–680.
26. Giroud, J.P. Development of criteria for geotextile and granular filters. In Proceedings of the 9th International Conference on Geosynthetics, Guarujá, Brazil, 23–27 May 2010; pp. 45–64.
27. Koerner, R.M.; Koerner, G.R. Lessons learned from geotextile filter failures under challenging field conditions. *Geotext. Geomembr.* **2015**, *43*, 272–281. [[CrossRef](#)]
28. Palmeira, E.M.; Trejos Galvis, H.L. Opening sizes and filtration behavior of nonwoven geotextiles under confined and partial clogging conditions. *Geosynth. Int.* **2017**, *24*, 125–138. [[CrossRef](#)]
29. Sousa, R.; Pinho-Lopes, M. Numerical tool for the design of granular and geotextile filters. In Proceedings of the 5th European Geosynthetics Congress, Valencia, Spain, 16–19 September 2012; pp. 274–283.
30. Wu, C.S.; Hong, Y.S.; Yan, Y.W.; Chang, B.S. Soil-nonwoven geotextile filtration behavior under contact with drainage materials. *Geotext. Geomembr.* **2006**, *24*, 1–10. [[CrossRef](#)]
31. Cazzuffi, D.; Moraci, N.; Mandaglio, M.C.; Ielo, D. Evolution in design of geotextile filters. In Proceedings of the 6th European Geosynthetics Congress, Ljubljana, Slovenia, 25–28 September 2016; pp. 40–63.
32. Miskowska, A.; Lenart, S.; Koda, E. Laboratory studies of artificial clogging of nonwoven geotextiles. In Proceedings of the 6th European Geosynthetics Congress, Ljubljana, Slovenia, 25–28 September 2016; pp. 1434–1440.
33. Segismundo, E.Q.; Kim, L.H.; Jeong, S.M.; Lee, B.S. A laboratory study on the filtration and clogging of the sand-bottom ash mixture for stormwater infiltration filter media. *Water* **2017**, *9*, 32. [[CrossRef](#)]
34. Maheshwari, B.K.; Gunjagi, D.A. Filtration and clogging behavior of geotextiles with roorkee soils. *Geotech. Geol. Eng.* **2008**, *26*, 101–107. [[CrossRef](#)]
35. Fannin, R.J. On the clogging of geotextile filters. In Proceedings of the 9th International Conference on Geosynthetics, Guarujá, Brazil, 23–27 May 2010; pp. 401–412.
36. Wesołowski, A.; Krzywosz, Z.; Brandyk, T. *Geosynthetics in Engineering Constructions*; SGGW: Warsaw, Poland, 2000; p. 70.
37. Fleming, I.R.; Rowe, R.K. Laboratory studies of clogging of landfill leachate collection and drainage systems. *Can. Geotech. J.* **2004**, *41*, 134–153. [[CrossRef](#)]

38. Adamcová, D.; Vaverková, M.D. New polymer behavior under the landfill conditions. *Waste Biomass Valoriz.* **2016**, *7*, 1459–1467. [[CrossRef](#)]
39. Koda, E.; Paprocki, P. Durability of leachate drainage systems of old sanitary landfills. In Proceedings of the 3rd International Conference Geofilters, Warsaw, Poland, 5–7 June 2000; pp. 215–222.
40. Correia, L.G.C.S.; Ehrlich, M.; Mendonca, M.B. The effect of submersion in the ochre formation in geotextile filters. *Geotext. Geomembr.* **2017**, *45*, 1–7. [[CrossRef](#)]
41. Yaman, C.; Martin, J.P.; Korkut, E. Effects of wastewater filtration on geotextile permeability. *Geosynth. Int.* **2006**, *13*, 87–97. [[CrossRef](#)]
42. Xue, Q.; Zhang, Q.; Liu, L. Impact of high concentration solutions on hydraulic properties of geosynthetic clay liner materials. *Materials* **2012**, *5*, 2326–2341. [[CrossRef](#)]
43. ISO 11058:2010—*Geotextiles and Geotextile-Related Products—Determination of Water Permeability Characteristics Normal to the Plane, Without Load*; International Organization for Standardization: Geneva, Switzerland, 2010.
44. ISO 14688-2:2004—*Geotechnical Investigation and Testing—Identification and Classification of Soil—Part 2: Principles for A Classification*; International Organization for Standardization: Geneva, Switzerland, 2004.
45. Kenney, T.C.; Lau, D. Internal stability of granular filters. *Can. Geotech. J.* **1985**, *22*, 215–225. [[CrossRef](#)]
46. Miskowska, A.; Koda, E.; Krzywosz, Z.; Król, P.; Boruc, N. Change of hydraulic properties of nonwoven geotextile after 22 years of exploitation in an earthfill dam. *Acta Sci. Pol.* **2016**, *15*, 119–126. (In Polish)
47. Koda, E.; Miskowska, A.; Stepień, S. Quality Control of Non-Woven Geotextiles Used in Drainage System in an Old Remedial Landfill. In Proceedings of the Geo-Chicago 2016, Chicago, IL, USA, 14–18 August 2016; pp. 254–263.
48. Kohata, Y.; Tanaka, M.; Sato, O.; Hirai, T. Clogging evaluation on cross-plane flow performance of geotextile filter. In Proceedings of the 8th International Conference on Geosynthetics, Yokohama, Japan, 18–22 September 2006; pp. 561–564.
49. Nishigata, T.; Fannin, R.J.; Vaid, Y.P. Blinding and clogging of a nonwoven geotextile. *Soils Found.* **2000**, *40*, 121–127. [[CrossRef](#)]
50. Lin, C.Y.; Yang, K.H. Experimental study on measures for improving the drainage efficiency of low-permeability and low-plasticity silt with nonwoven geotextile drains. *J. Chin. Inst. Civ. Hydraul. Eng.* **2014**, *26*, 71–82.
51. Miskowska, A. Tests of the influence of clogging on the filtration properties of nonwoven geotextiles. In *Outline of Selected Issues in Land Engineering*; Bzówka, J., Ed.; Silesian University of Technology: Gliwice, Poland, 2016; pp. 51–58. (In Polish)
52. Chen, R.H.; Ho, C.C.; Chung, W.B. The filtration mechanism and micro-observation of soil-geotextile systems under cyclic flows. *J. Geoen.* **2008**, *3*, 101–112.
53. Faure, Y.H.; Ho, C.C.; Chen, R.H.; Lay, M.; Blaza, J. A wave flume experiment for studying erosion mechanism of revetments using geotextiles. *Geotext. Geomembr.* **2010**, *28*, 360–373. [[CrossRef](#)]

